PAPER

NJC
www.rsc.org/njc

Paramagnetic transition metal complexes with a redox-active ligand: $M(hfac)_2(EDO\text{-}EDT\text{-}TTF\text{-}py)_n$; [M = Cu^{II}, n = 1, 2; M = Mn^{II}, n = 2]†

Akira Ota,[ab] Lahcène Ouahab,*[a] Stéphane Golhen,[a] Olivier Cador,[a] Yukihiro Yoshida[b] and Gunzi Saito[b]

[a] *Laboratoire de Chimie du Solide et Inorganique Moléculaire, UMR 6511 CNRS-Université de Rennes 1, Institut de Chimie de Rennes, Campus Beaulieu, 35042 Rennes Cedex, France. E-mail: lahcene.ouahab@univ-rennes1.fr; Fax: +33 (0)2 23 23 68 40; Tel: +33 (0)2 23 23 56 59*

[b] *Division of Chemistry, Graduate School of Science, Kyoto University, Kyoto, 606-8502, Japan*

Received (in Montpellier, France) 20th May 2005, Accepted 21st June 2005
First published as an Advance Article on the web 14th July 2005

Synthesis, crystal structures, electrochemical and physical properties of the new ligand, EDO-EDT-TTF-py (**L1**) [4,5-ethylenedioxy-4′,5′-(4-pyridylethylenedithio)tetrathiafulvalene], and the paramagnetic transition metal coordination complexes, $M(hfac)_2(EDO\text{-}EDT\text{-}TTF\text{-}py)_2$; M = Cu^{II} (**2**), Mn^{II} (**3**), and $Cu^{II}(hfac)_2$(EDO-EDT-TTF-py) (**4**) are reported where hfac = hexafluoroacetylacetonato. Crystal data: (**L1**) triclinic system, space group $P\bar{1}$, a = 8.4060(3), b = 10.5093(3), c = 11.5318(5) Å, α = 64.758(2), β = 86.923(2), γ = 72.444(2)°, V = 875.22(6) Å^3, Z = 2, **2** and **3** are isostructural (data for **3** are given in brackets), triclinic system, space group $P\bar{1}$, a = 7.1085(4) [7.1013(9)Å], b = 11.1210(7) [11.111(2)Å], c = 16.3628(11) Å [16.346(3) Å], α = 91.682(2) [91.662(6)], β = 91.014(3) [91.036(7)], γ = 93.547(3)° [93.651(6)°], V = 1290.3(1) Å^3 [1286.3(3) Å^3], Z = 1, (**4**) triclinic system, space group $P\bar{1}$, a = 9.2937(1), b = 15.1897(2), c = 24.3174(6) Å, α = 92.461(1), β = 93.048(1), γ = 105.491(1)°, V = 3297.6(1) Å^3, Z = 4.‡ In the compounds **2**, **3** and **4**, the ligand **L1** is coordinated to the transition metals through the nitrogen atom of the pyridine group. In the crystal, the organic and inorganic layers are segregated. The arrangement of the organic layers is similar to the well known β phase in BEDT-TTF [bis(ethylenedithio)tetrathiafulvalene] charge transfer complexes, showing that the crystal packing is mainly governed by π–π stacking of the organic molecules. **L1** is a TTF derivative and shows the electron donating ability with oxidation potential $E_1^{\frac{1}{2}}$ = +0.52 V *versus* SCE in benzonitrile. The same oxidation potentials were observed for complexes **2** and **3**, indicating the negligible interactions between the ligands and the metals in solution.

Introduction

Numerous Charge Transfer (CT) complexes based on organic donors such as TTF (tetrathiafulvalene) and the derivatives have been intensively studied.[1] The (super)conducting and magnetic properties of these CT complexes have been revealed, and the coexistence or correlation of conductivity with magnetism is a current intense interest both in terms of the basic science and application for the electronic devices.[2] The well examined strategy to combine electrical conductivity and magnetism is the association of electron donor molecules as radical cations and magnetic counter anions in CT salts.[3] In this case, the stacks or layers of the donor molecule are crucial for the conducting property, and the anions are the main source of magnetic property. The interactions between the donor and anion can be realized through the overlaps of the molecular orbitals derived from the intermolecular atomic contacts. However, these interactions are weak in general.

Another approach is to establish interactions between the donor molecules and magnetic transition metals through the coordination bonds.[4–11] Some TTF derivatives bearing functional groups with coordination ability have been synthesized and their paramagnetic transition metal coordination complexes have been prepared.[4–11] The important process is to oxidize TTF derivative ligands in the coordination complexes associated with the generation of the conducting carrier in the crystals.[6,7] Although few complexes were successfully oxidized, it showed an insulating behavior due to the dimerization[6] and lack of stacking[7] in the donor sublattice.

Continuing our efforts for the development of materials in which conductivity and magnetism coexist and correlate, we investigate the coordination complexes of EDO-EDT-TTF-py (4,5-ethylenedioxy-4′,5′-(4-pyridylethylenedithio)TTF) (**L1**) which is a derivative of EDO-EDT-TTF (4,5-ethylenedioxy-4′,5′-ethylenedithio-TTF).[11] EDO-EDT-TTF as well as the other donor molecule containing ethylenedioxy groups *i.e.* BEDO-TTF (bis(ethylenedioxy)-TTF)[12] affords a number of conducting CT complexes by the self-assembling ability derived from the ethylenedioxy groups. In this paper, we report the synthesis and crystal structures of the new ligand EDO-EDT-TTF-py (**L1**) and three of its coordination complexes, $M(hfac)_2$(**L1**)$_2$; M = Cu^{II} (**2**), Mn^{II} (**3**), hfac = hexafluoroace-

† Electronic supplementary information (ESI) available: detailed X-ray structural data including crystallographic parameters, atomic coordinates, bond distances and angles, anisotropic thermal parameters, and H atom coordinates for **L1**, **2**, **3** and **4** as CIF file; charts of cyclic voltametry for **L1**, **2**, and **3**; UV-Vis-IR spectra for **L1**, **2**, **3**; χT *vs.* T plots for **2** and **3**; ESR spectra for **2** and **3**. See http://dx.doi.org/10.1039/b507163a

‡ CCDC reference numbers 275856–275859. See http://dx.doi.org/10.1039/b507163a for crystallographic data in CIF or other electronic format.

DOI: 10.1039/b507163a

tylacetonato and Cu(hfac)$_2$(**L1**). [M(hfac)$_2$] blocks have been already used as efficient components for magnetic materials, for instance with organic radicals of nitroxide derivatives coordinated to metal ions.[13] Electrochemical study and other physical properties of **L1**, **2–3** are also reported.

Experimental

General

^{1}H NMR was recorded on a Bruker AC 300P spectrometer. Chemical shifts are reported in parts per million referenced to TMS for ^{1}H NMR. Melting points were measured using a Yanaco MP-500D without correction. Elemental analyses results were obtained from the Laboratoire Central de Microanalyse du CNRS, Lyon, France. Mass spectra were recorded with a JMS-AM II 120 (JEOL) instrument. Cyclic voltametry was carried out in benzonitrile solution, containing 0.1 M $N(C_4H_9)_4BF_4$ as the supporting electrolyte. Voltamograms were recorded at 10 mV s^{-1} at a platinum disk electrode. The potentials were measured *versus* a saturated calomel electrode (SCE). Optical spectra were measured using the KBr disk method on Perkin–Elmer 1600 Series FT-IR (resolution 4 cm^{-1}) for infrared (IR) and near-infrared region (400–7800 cm^{-1}) and on a SHIMADZU UV-3100 spectrometer for near-infrared, visible, and ultraviolet (UV-Vis-NIR) region (3800–42000 cm^{-1}). A Quantum Design MPMS-XL SQUID magnetometer was used to collect magnetization data from 2 K to 300 K. The polycrystalline sample (*ca.* 10–15 mg) wrapped by polyethylene film was placed inside a polyethylene straw. The conductivity was measured with a powdered sample which is packed in a Teflon tube by two probe method using stainless electrodes. X-band ESR spectra were recorded at room temperature for the powder samples of **2** and **3** with a JEOL JES TE-200 X-band spectrometer equipped with TE_{011} cavity.

Synthesis

All solvents were dried using standard procedures. Cu(hfac)$_2 \cdot x$H$_2$O ($x \sim 2$) and Mn(hfac)$_2 \cdot 3$H$_2$O were purchased from Aldrich Co. Ltd and were used without further purification. Triethylphosphite was used as purchased. 4,5-Ethylenedioxy-1,3-dithiol-2-thion (**1a**) and 4,5-(4-pyridylethylenedithio)-1,3-dithiole-2-one (**1b**) were synthesized by modified methods described in refs. 10 and 14, respectively.

4,5-Ethylenedioxy-4′,5′-(4-pyridylethylenedithio)tetrathiafulvalene (EDO-EDT-TTF-py) (L1). **1a** (1.0 g, 5.2 mmol) and **1b** (1.0 g, 3.5 mmol) were suspended in a mixture of triethylphosphite (80 mL) and toluene (30 mL). The mixture was put into oil bath at 120 °C under argon atmosphere and stirred for 2 h. The resulting mixture was cooled to room temperature (RT) and left in a refrigerator. The obtained yellow precipitate was filtered, washed with methanol and recrystallized from dichloromethane and methanol to give **L1** as yellow plate crystals (0.9 g, 2.1 mmol, 60% yield based on **1b**). **1**: mp 167.0–168.0 °C (decomp.); δ_H ($CDCl_3$): 3.41 (2H, d), 4.27 (4H, s), 4.62 (1H, dd), 7.29 (2H, d), 8.62 (2H, d); MS *m*/*z* 431, 430 (M^+), 429. Anal. calcd for $C_{15}H_{11}NO_2S_6$: C, 41.93; H, 2.58; N, 3.26; O, 7.45. Found: C, 41.76; H, 2.46; N, 3.60; O, 7.14%.

Cu^{II}(hfac)$_2$(L1)$_2$ (2) and Cu^{II}(hfac)$_2$(L1) (4). CH_2Cl_2 solution (70 mL) of **L1** (170 mg, 0.40 mmol) was put into a hexane solution (60 mL) of Cu^{II}(hfac)$_2 \cdot x$H$_2$O (100 mg, 0.20 mmol) under reflux. The solution was kept under reflux for a further 15 minutes and cooled to RT. The solvents were slowly evaporated and red plate crystals of **2** appeared. The crystals (130 mg, 0.10 mmol, 50% yield based on **L1**) were filtered and washed with hexane. From the filtered solution, dark green block crystals of Cu^{II}(hfac)$_2$(**L1**) (**4**) were obtained with further evaporation of the solvents and were picked out using a wooden stick for the crystal structure analysis. **2**: Anal. calcd for $C_{40}H_{24}N_2O_8S_{12}F_{12}Cu$: C, 35.94; H, 1.81; N, 2.10. Found: C, 35.93; H, 1.98; N, 2.41%. The stoichiometry of (**4**) is determined from the X-ray crystal structure analysis.

Mn^{II}(hfac)$_2$(L1)$_2$ (3). A CH_2Cl_2 solution (70 mL) of **L1** (160 mg, 0.37 mmol) was added to a hexane solution (60 mL) of Mn(hfac)$_2 \cdot 3$H$_2$O (100 mg, 0.19 mmol) under reflux. The solution was kept under reflux for further 15 minutes and then cooled to RT. The solvents were slowly evaporated and pale red plate crystals of **3** appeared. The crystals were filtered and washed with hexane (193 mg, 0.15 mmol, 79% based on **L1**). **3**: Anal. calcd for $C_{40}H_{24}N_2O_8S_{12}F_{12}Mn$: C, 36.13; H, 1.81; N, 2.11. Found: C, 35.62; H, 1.91; N, 2.22%.

X-ray crystallography

Single-crystal diffraction data were collected on a Kappa diffractometer equipped with a CCD detector from the Centre de Diffractométrie X (CDFIX), Université de Rennes 1, France. Structures were solved with SHELXS-97 and refined with SHELXL-97 programs by full matrix least squares method on F^2.[15] Crystallographic data are summarized in Table 1. The poor accuracy, especially for **3**, is due to bad crystal quality, however, one can see that compounds **2** and **3** are isostructural. Atomic coordinates and complete crystal structure results are given as supplementary material.†

Results and discussion

Synthesis

4,5-Ethylenedioxy-4′,5′-(4-pyridylethylenedithio)tetrathiafulvalene (L1). The phosphite cross coupling reaction (Scheme 1) affords compound **L1** as yellow crystals in relatively good yield (60%). This yield is larger than that of 26% obtained in the same kind of reaction for 4,5-ethylenedithio-4′,5′-(4-pyridylethylenedithio)tetrathiafulvalene (BEDT-TTF-py, Scheme 2),[10] and it is close to the value of 57% for ethylenedioxy-*S*,*S*-dimethylethylenedithiotetrathiafulvalene (EDO-*S*,*S*-DMEDT-TTF).[16] **L1** has a chirality derived from the connection between EDO-EDT-TTF part and the pyridine group, the racemic compound was then obtained in this reaction as shown from the crystal structure analysis (see below).

Cu^{II}(hfac)$_2$(L1)$_2$ (2) and Cu^{II}(hfac)$_2$(L1) (4). Cu^{II}(hfac)$_2$ possesses two more sites which are open to other ligands for the hexa-coordinated state. Compound **2** was obtained by the modified method used in the synthesis of Cu^{II}(hfac)$_2$(TTF-CHCH-py)$_2$.[5] Both **2** and **4** were identified by X-ray crystal structure analysis. The red and dark green colors of the crystals in **2** and **4** respectively are derived from the different ligand fields in each compound, since Cu atom in **2** is hexa-coordinated and penta-coordinated in **4**.

Mn^{II}(hfac)$_2$(L1)$_2$ (3). The hexa-coordinated complex **3** was obtained by the same method used for **2**, with a higher yield (79%) than for **2**. No penta-coordinated Mn^{II}(hfac)$_2$(L1) complex was obtained.

All the attempts to prepare radical cation salts of these complexes either by electrocrystallization or chemical oxidation have been unsuccessful to date.

Crystal structures

EDO-EDT-TTF-py (L1). Crystallographic data and selected bond lengths of **L1**, **2–4** are shown in Tables 1 and 2, respectively. ORTEP drawing of the molecular structure at RT for **L1** with the atomic numbering scheme is shown in

Table 1 Crystallographic data for compounds **L1**, **2**, **3** and **4**

	L1	**2**	**3**	**4**
Chemical Formula	$C_{15}H_{11}NO_2S_6$	$C_{40}H_{24}CuF_{12}N_2O_8S_{12}$	$C_{40}H_{24}MnF_{12}N_2O_8S_{12}$	$C_{25}H_{13}CuF_{12}NO_6S_6$
FW	429.61	1336.87	1328.27	907.26
Cryst. system	Triclinic	Triclinic	Triclinic	Triclinic
Space group	$P\bar{1}$	$P\bar{1}$	$P\bar{1}$	$P\bar{1}$
a/Å	8.4060(3)	7.1085(4)	7.1013(9)	9.2937(1)
b/Å	10.5093(3)	11.1210(7)	11.111(2)	15.1897(2)
c/Å	11.5318(5)	16.3628(11)	16.346(3)	24.3174(6)
α/°	64.758(2)	91.682(2)	91.662(6)	92.461(1)
β/°	86.923(2)	91.014(3)	91.036(7)	93.048(1)
γ/°	72.444(2)	93.547(3)	93.650(6)	105.491(1)
V/Å^3	875.22(6)	1290.3(1)	1286.3(3)	3297.6 (1)
μ/cm^{-1}	7.90	10.04	8.39	11.52
Z	2	1	1	4
No. of reflns.	6367	10073	9051	22 071
No. of unique reflns.	3961	4743	3500	12 843
R_{int}	0.0260	0.0819	0.1496	0.0365
R_1 [$Fo^2 > 2\sigma(Fo^2)$]^a	0.050 [2953]	0.082 [2817]	0.105 [1522]	0.063 [8037]
wR_2 (Fo^2)^b	0.123	0.222	0.264	0.155

^{a} $R_1 = \sum\|Fo| - |Fc\|/\sum |Fo|$. ^{b} $wR_2 = \{\sum[w\,(Fo^2 - Fc^2)^2]/\sum[w\,(Fo^2)^2]\}^{1/2}$.

Fig. 1. There is one crystallographically independent molecule generating two molecules in the unit cell. The molecules are related by the center of inversion which yields one molecule as *S*- and the other molecule as *R*-isomer, resulting in the racemic compound.[9] EDO-EDT-TTF moiety and pyridine group are not coplanar with a dihedral angle of *ca.* 80.1(1)°. EDO-EDT-TTF moiety shows a boat conformation (Fig. S1, see ESI†), which is typical for a neutral TTF derivative molecule. No intermolecular atomic contact shorter than the sum of van der Waals radii was observed.

Pyridine and its derivatives have been widely used as ligand in coordination complexes with various transition metals.[4–10] The pyridine group in **L1** has also a potential coordinating ability as in 4-(2-tetrathiafulvalenylethenyl)pyridine (TTF-CHCH-py, Scheme 2).[4–6] In the case of TTF-CHCH-py, the whole molecule is a π-conjugated system with flat molecular shape, whereas the π-conjugation between the EDO-EDT-TTF moiety and the pyridine group is lost through the distorted shape in **L1**.

Another feature of **L1** is the extended π-conjugated system in the donor moiety. Addition of further peripheral chalcogen atoms to the TTF skeleton is expected to increase the dimensionality of the electronic structure in the oxidized complex.[1]

TTF derivatives with the coordination ability have been reported, some of which have the multi-coordination sites,[7–9] while **L1** and TTF-CHCH-py have only one nitrogen atom as coordination site. When multidentate ligands are attached to a transition metal, the magnetic interaction might be optimized between the molecule and transition metal, however, the structure around the transition metal is firmly fixed, which may restrict the π–π stacks in the donor parts. **L1** has structural flexibility, since **L1** has only one site for coordination and the flexible single bond between EDO-EDT-TTF moiety and pyridine group enable various coordination patterns in the complexes.

M(hfac)$_2$(L1)$_2$; M = Cu^{II} (2), Mn^{II} (3). Compounds **2** and **3** are isostructural, and thus we describe only the structure of **2** and give the corresponding values for **3** in brackets for comparison. The molecular structure of **2** with the atomic numbering scheme is shown in Fig. 2. The metal atom is located on a center of inversion and therefore the asymmetric unit consists of a half molecule of the complex. The M^{II} is coordinated to the oxygen atoms from two bidentate hfac$^-$ anions and two nitrogen atoms from the pyridine groups of **L1** as an octahedral coordination geometry (see Table 2).

The distance between the metal and O3 is longer than the other coordination bonds and the bond angles around the metal atom slightly deviate from 90° (see Table 2). The two **L1** ligands are related by a center of inversion and therefore the *R*- and *S*-isomers coexist in a molecule. As in the non-coordinated ligand **L1**, the EDO-EDT-TTF moiety and pyridine group are not coplanar, the dihedral angle being equal to 85.38(23)°[84.65(40)°]. EDO-EDT-TTF moiety, which is deformed in **L1**, is almost flat in **2** (Fig. 3a).

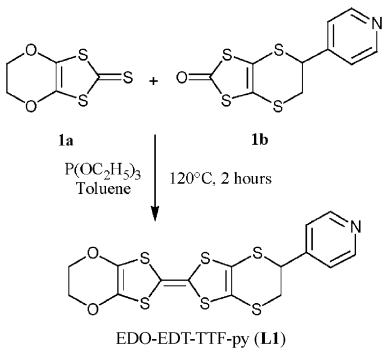

Scheme 1 Synthesis of **L1**.

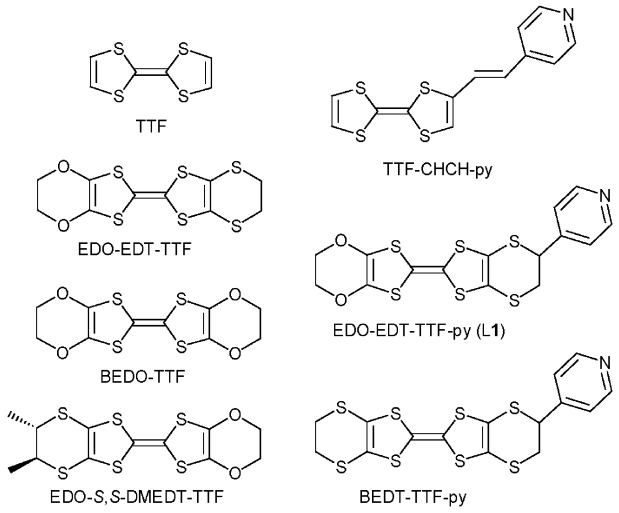

Scheme 2 TTF derivatives (see text).

Table 2 Selected bond length in Å for **L1**, **2**, **3** and **4**; Selected bond angles in deg. for **2**, **3** and **4**

	L1	**2**	**3**		**4**	
					A Molecule (x = a)	B Molecule (x = b)
C10–C11	1.346(4)	1.352(9)	1.336(18)	S4x-C10x	1.752(5)	1.753(5)
S4–C10	1.756(3)	1.744(7)	1.747(13)	S4x-C9x	1.761(5)	1.747(5)
S4–C9	1.761(3)	1.728(7)	1.732(15)	S3x-C10x	1.753(5)	1.762(5)
S6–C13	1.754(3)	1.750(8)	1.724(16)	S3x-C8x	1.756(5)	1.755(5)
S6–C11	1.757(3)	1.736(7)	1.745(14)	S6x-C13x	1.756(6)	1.756(6)
S3–C10	1.754(3)	1.750(7)	1.726(14)	S6x-C11x	1.757(5)	1.758(5)
S3–C8	1.762(3)	1.727(7)	1.709(13)	S5x-C12x	1.759(6)	1.757(6)
S5–C12	1.750(3)	1.754(7)	1.726(15)	S5x-C11x	1.759(6)	1.761(5)
S5–C11	1.756(3)	1.756(8)	1.777(14)	C12x-C13x	1.319(8)	1.318(8)
C8–C9	1.346(4)	1.348(10)	1.358(18)	C10x-C11x	1.351(7)	1.345(7)
C13–C12	1.323(4)	1.295(11)	1.278(19)	C8x-C9x	1.337(7)	1.344(7)
M–N1		2.018(5)	2.046(11)	Cu1x-O6x	1.939(4)	1.961(4)
M–O3		2.285(5)	2.278(9)	Cu1x-O3x	1.950(3)	1.954(4)
M–O4		1.986(5)	2.006(9)	Cu1x-O4x	1.956(4)	1.950(4)
				Cu1x-N1x	1.982(4)	1.990(4)
				Cu1x-O5x	2.200(4)	2.239(4)
O4–M–N1		90.7(2)	90.6(4)	O6x-Cu1x-O3x	174.54(17)	173.36(18)
O4–M–N1		89.3(2)	89.4(4)	O6x-Cu1x-O4x	85.03(17)	85.09(17)
O4–M–O3		92.86(19)	92.7(4)	O3x-Cu1x-O4x	90.65(16)	89.46(17)
N1–M–O3		92.02(19)	91.8(4)	O6x-Cu1x-N1x	91.89(17)	92.75(17)
O4–M–O3		87.14(19)	87.3(4)	O3x-Cu1x-N1x	91.71(16)	92.18(17)
N1–M–O3		87.98(19)	88.2(4)	O4x-Cu1x-N1x	168.75(18)	172.67(18)
				O6x-Cu1x-O5x	89.42(15)	85.81(15)
				O4x-Cu1x-O5x	91.71(18)	90.19(16)
				O3x-Cu1x-O5x	94.06(16)	98.03(16)
				N1x-Cu1x-O5x	99.09(16)	96.65(16)

The bond lengths of the coordinated and non-coordinated **L1** ligands are very close to each other, indicating that the two ligands in **2** and **3** are neutral,[17] since the charge is balanced between the metal (M^{II}) and ($hfac^{-}$)$_2$. F atoms of hfac units show relatively large thermal factors which are usually observed for other compounds containing the hfac unit at RT.[5,6]

EDO-EDT-TTF moieties form uniform stacking columns with the distance of 4.0 Å between the stacked molecular planes (Fig. 3a). Inter-column S···S atomic contacts shorter than the sum of van der Waals radii (dashed lines in Fig. 3b, S6–S6: 3.323 Å; S1–S5: 3.541 Å) were observed. Thus EDO-EDT-TTF moiety forms two-dimensional layered structure in the *ab* plane (Fig. 3b), which is similar to the *β*-type packing observed in some BEDT-TTF (CT) salts.[1] This type of packing is suitable for electrical conductivity, when the conducting carriers are introduced in the layer by the (electro)chemical oxidation and/or electronic field as the field effect transistor.[18] M(hfac)$_2$ part also forms a layered structure and the organic and inorganic layers stack alternately along the *c* axis. The tight packing in the organic layer gives rise to the flat organic molecules, showing the structural flexibility of the EDO-EDT-TTF moiety.

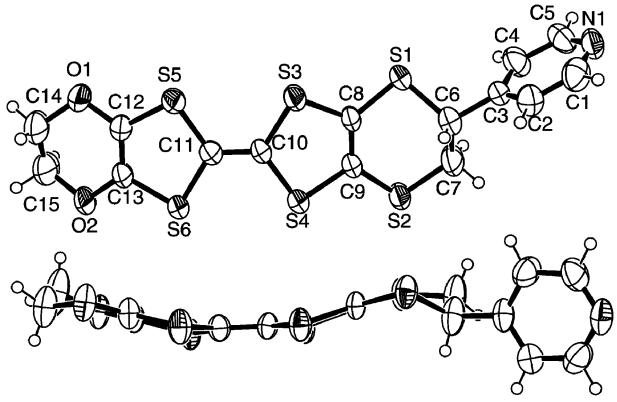

Fig. 1 ORTEP drawing for **L1** showing the atomic numbering scheme (up), and the side view (down).

$Cu^{II}(hfac)_2$(L1) (4). The molecular structure of **4** consists of two independent $Cu^{II}(hfac)_2$(L1) molecules named A and B. The atomic numbering scheme is shown in Fig. 4a. The EDO-EDT-TTF moiety and pyridine group are not coplanar with a dihedral angle of 72.67(12)° for molecule A and 78.05(13)° for molecule B. In this complex the Cu atom is penta-coordinated, since the molecule has one **L1** and two hfac as the ligands. Compound **4** is racemic, since one molecule includes *S*- and the other molecule includes *R*-EDO-EDT-TTF-py as the crystallographically independent molecules. The distance between Cu1a and O5a in A (Cu1b and O5b in B) is longer than the other coordination bonds, showing the distorted pyramidal coordination. EDO-EDT-TTF moiety shows a boat conformation as that of **L1** (Fig. 4b).

EDO-EDT-TTF moiety forms the two-dimensional layered structure (Fig. 5), and no inter-molecular S···S atomic contact was observed in the layer. The crystal structure consists of the alternate layers of the EDO-EDT-TTF part and doubly stacked Cu(hfac)$_2$ along the *c*-axis.

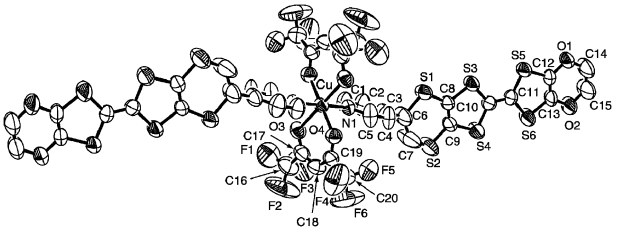

Fig. 2 ORTEP drawing for **2** showing the atomic numbering scheme, H atoms are omitted for clarity.

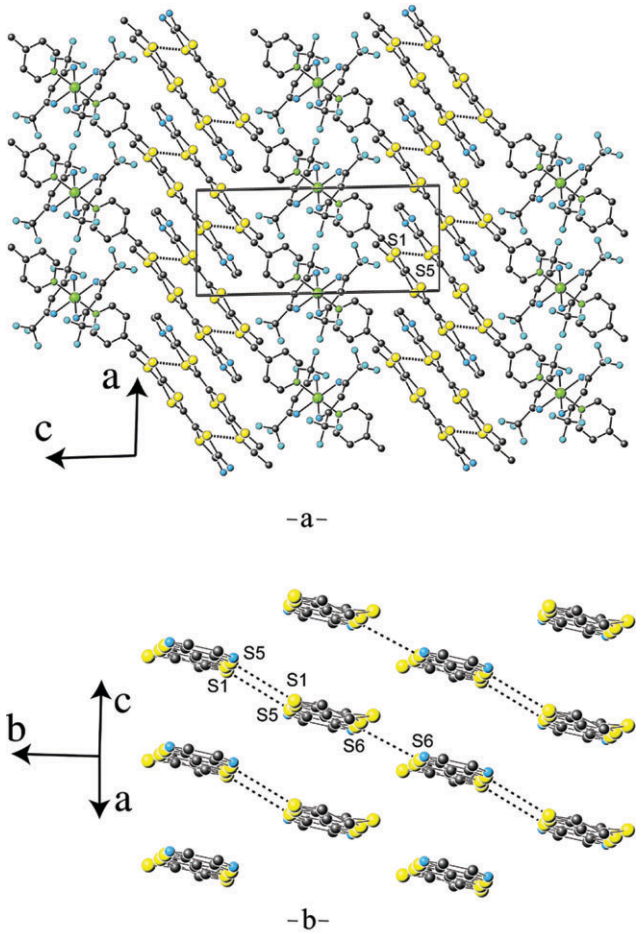

Fig. 3 Crystal structure of **2**, (a) viewed along the *b*-axis, and (b) layer of donor part viewed along the molecular long axis of EDO-EDT-TTF moiety. Dashed lines correspond to S–S intermolecular contacts shorter than the sum of van der Waals radii, H atoms are omitted for clarity.

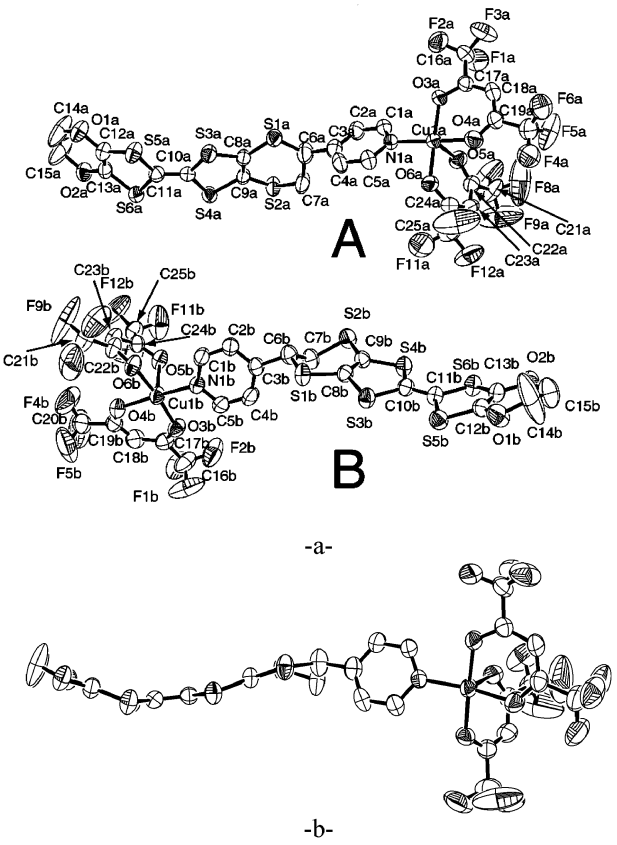

Fig. 4 (a) ORTEP drawing for **4** showing the atomic numbering scheme for molecules A and B. (b) Side view of A molecule, H atoms are omitted for clarity.

Electrochemical study

Cyclic voltamograms are given as supplementary material (Fig. S2 and Fig. S3, see ESI†) and the redox potentials are displayed in Table 3 together with those of BEDT-TTF, and EDO-EDT-TTF for comparison. The reversible redox waves were observed in benzonitrile, while the measurements in dichloromethane and 1,2-dichloroethane show irreversible waves for **2** and **3**. This difference may be caused by the precipitation of the radical cation salts of **2** and **3** on the electrode in the case of dichloromethane and 1,2-dichloroethane.

As for **L1**, two reversible single-electron redox waves were observed as $E_1^{1/2}$ and $E_2^{1/2}$. The values are slightly larger than those of EDO-EDT-TTF, showing that **L1** has the electron donating ability as TTF derivatives. In the chart of **2** and **3**, two reversible single-electron redox waves which obviously correspond to those of **L1** were observed. Hence the coordinated EDO-EDT-TTF-py moieties in **2** and **3** keep the electron donating ability just the same as the non-coordinated unit **L1**, and *R*-and *S*-EDO-EDT-TTF-py moieties are oxidized independently.

Table 3 Data of cyclic voltammograms in 0.1 M $N(C_4H_9)_4BF_4$/benzonitrile on a Pt disc electrode *vs.* SCE

	$E_1^{1/2}$/V	$E_2^{1/2}$/V	$E_2^{1/2} - E_1^{1/2}$/V
L1	+0.52	+0.83	+0.31
2	+0.52	+0.83	+0.31
3	+0.52	+0.83	+0.31
BEDT-TTF	+0.62	+0.92	+0.30
EDO-EDT-TTF	+0.49	+0.81	+0.32

Physical properties

The UV-Vis-IR spectrum of **L1** (Fig. S4, see ESI†) shows absorption bands at 19.7 × 10^3 cm^{-1}, 27.0 × 10^3 cm^{-1} and 30.1 × 10^3 cm^{-1}, corresponding to the bands of BEDO-TTF.[12] The spectrum of **2** (Fig. S4, see ESI†) shows the same three absorption bands and another band appears at 11.0 × 10^3 cm^{-1}. The additional band is due to a d–d transition of Cu^{II}. The spectrum of **3** (Fig. S4, see ESI†) shows the same spectral feature of **L1**, since the d–d transitions of Mn^{II} are spin-forbidden.[19]

The temperature dependencies of the magnetic susceptibility for **2** and **3** were measured in the temperature range 2–300 K, with an applied field of 0.1 T (Fig. S5, see ESI†). In both compounds **2** and **3**, the susceptibility indicates a Curie–Weiss law with the weak magnetic interaction ($\Theta = -1.0$ K for **2** and −1.8 K for **3**). The Curie constant C for **2** is 0.48 cm^3 K mol^{-1} which is higher than the spin-only value 0.38 cm^3 K mol^{-1} for non-interacting d-electron spin ($S = 1/2$) of Cu^{II}. For compound **3**, C is 4.62 cm^3 K mol^{-1} which is higher than the spin-only value 4.38 cm^3 K mol^{-1} for non-interacting d-electron spin ($S = 5/2$) of Mn^{II} high spin. The origin of the magnetism in **2** and **3** was examined in the ESR spectra at room temperature (Fig. S6, see ESI†). The spectrum of **2** shows broad multiple signals at g ∼ 2 derived from the d-electron spin of Cu^{II}. The spectrum of **3** consists of broad asymmetric signals which are derived from the d-electron spin of Mn^{II}. The shortest M···M distance is 7.1 Å and no other source of spin exists in these compounds, and thus the intermolecular magnetic interactions are very weak.

The conductivities of **L1**, **2**, **3** were measured on the compressed pellets by the two-probes method at RT and, as

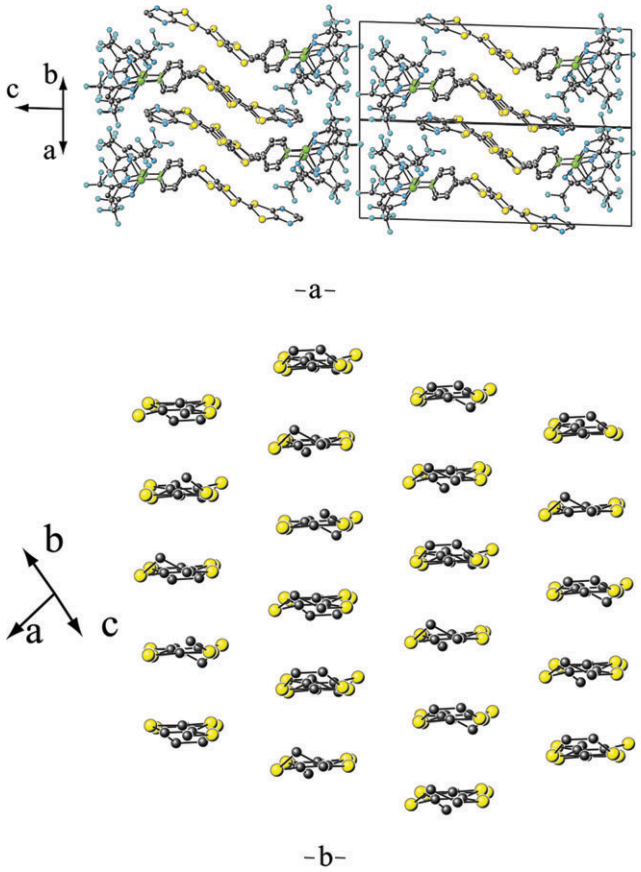

Fig. 5 (a) Crystal structure of **4** viewed along the *b*-axis. (b) Donor stacking viewed along the molecular long axis of EDO-EDT-TTF moiety.

expected, both compounds are insulators ($\rho > 3.1 \times 10^8\ \Omega$ cm) for **L1** and **3**, $\rho = 1.6 \times 10^8\ \Omega$ cm for **2**.

Conclusion

The electron donor molecule (**L1**) with coordination ability was successfully synthesized and characterized. Its coordination complexes (**2**, **3**, **4**) with paramagnetic transition metal ions were prepared. Compounds **2** and **3** are electron donors with oxidation potentials comparable to those of **L1**. Static susceptibility data, ESR and conductivity of **2** and **3** are in agreement with the neutral state of **L1**. The crystal structures of **2–4** are characterized by segregated organic and inorganic 2-D layers reminiscent of those usually observed in conducting and superconducting organic materials. This demonstrates that the extension of the π-system is effective for building layered structures even in coordination systems. In **2–4**, the **L1** donor ligands shows the well-known two-dimensional *β*-type of packing. This kind of molecular arrangement is suitable for conducting path. However, in these compounds, the EDO-EDT-TTF moieties are neutral and consequently these compounds are insulators. In order to achieve electrical conductivity, the organic ligands must be partially oxidized. In this case, two kinds of spins coexist in the crystal. Thus one can expect a magneto resistance effect caused by the molecular field arising from the spins of the transition metal. Efforts to prepare radical cation salts of these new complexes are continuing.

Acknowledgements

This work was in part supported by the CNRS-JSPS project PICS No 1433, a Grant-in-Aid for JSPS fellows, a COE Research on Elements Science (No. 12CE2005), a Grant-in-Aid (21st Century COE program on Kyoto University Alliance for Chemistry), and the Grant-in-Aid for Scientific Research (No. 15205019 by JSPS).

References

1 (*a*) T. Ishiguro, K. Yamaji and G. Saito, *Organic Superconductors*, Springer-Verlag, Heidelberg, Germany, 1998; (*b*) J. M. Williams, J. R. Ferraro, R. J. Thorn, K. D. Carlson, U. Geiser, H. H. Wang, A. M. Kini and M. H. Whangbo, in *Organic Superconductors. Synthesis, Structure, Properties and Theory*, ed., R. N. Grimes, Prentice Hall, Englewood Cliffs, New Jersey, 1992.
2 L. Ouahab and E. Yagubskii, *Organic Conductors Superconductors and Magnets: from Synthesis to Molecular Electronics*, NATO-ASI Series, Kluwer, 2004, vol II, 139.
3 (*a*) A. W. Graham, M. Kurmoo and P. Day, *J. Chem. Soc., Chem. Commun.*, 1995, 2061; (*b*) A. Kobayashi, T. Udagawa, H. Tomita, T. Naito and H. Kobayashi, *Chem. Lett.*, 1993, 2179; (*c*) H. Kobayashi, A. Kobayashi and P. Cassoux, *Chem. Soc. Rev.*, 2000, **29**, 325; (*d*) E. Coronado, J. R. Galan-Mascaros and C. J. Gomez-Garcia, *Nature*, 2000, **408**, 447; (*e*) L. Ouahab, *Chem. Mater.*, 1997, **9**, 1909.
4 F. Iwahori, S. Golhen, L. Ouahab, R. Carlier and J. P. Sutter, *Inorg. Chem.*, 2001, **40**, 6541.
5 L. Ouahab, F. Iwahori, S. Golhen, R. Carlier and J. P. Sutter, *Synth. Met.*, 2003, **505**, 133–134.
6 F. Setifi, L. Ouahab, S. Golhen, Y. Yoshida and G. Saito, *Inorg. Chem.*, 2003, **42**, 1791.
7 N. Avarvari and M. Fourmigué, *Chem. Commun.*, 2004, 1300.
8 (*a*) P. Pellon, G. Gachot, J. Le Bris, S. Marchin, R. Carlier and D. Lorcy, *Inorg. Chem.*, 2003, **42**, 2056; (*b*) C. E. Uzelmeier, S. L. Bartley, M. Fourmigué, R. Rogers, G. Grandinetti and K. R. Dunbar, *Inorg. Chem.*, 1998, **37**, 6706; (*c*) S. -X. Liu, S. Dolder, M. Pilkington and S. Decurtins, *J. Org. Chem.*, 2002, **67**, 3160.
9 C. Réthoré, M. Fourmigué and N. Avarvari, *Chem. Commun.*, 2004, 1384.
10 W. Xu, D. Q. Zhang, H. X. Li and D. B. Zhu, *J. Mater. Chem.*, 1999, **9**, 1245.
11 G. Saito, H. Sasaki, T. Aoki, Y. Yoshida, A. Otsuka, H. Yamochi, O. O. Drozdova, K. Yakushi, H. Kitagawa and T. Mitani, *J. Mater. Chem.*, 2002, **6**, 1640.
12 S. Horiuchi, H. Yamochi, G. Saito, K. Sakaguchi and M. Kusunoki, *J. Am. Chem. Soc.*, 1996, **118**, 8604.
13 A. Caneschi, D. Gatteschi and R. Sessoli, *Acc. Chem. Res.*, 1989, **22**, 392.
14 M. Iyoda, Y. Kuwatani, E. Ogura, K. Hara, H. Suzuki, T. Takano, K. Takeda, J. Takano, K. Ugawa, M. Yoshida, H. Matsuyama, H. Nishikawa, I. Ikemoto, T. Kato, N. Yoneyama, J. Nishijo, A. Miyazaki and T. Enoki, *Heterocycles*, 2001, **54**, 833.
15 G. M. Sheldrick, *SHELX-97, Program for crystal structure refinement*, University of Göttingen, Germany, 1997.
16 T. Konoike, K. Namba, T. Shinada, K. Sakaguchi, G. C. Papavassiliou, K. Murata and Y. Ohfune, *Synlett.*, 2001, 1476.
17 P. Guionneau, C. J. Kepert, G. Bravic, D. Chasseau, M. R. Truter, M. Kurmoo and P. Day, *Synth. Met.*, 1997, **86**, 1973.
18 A. Tsumura, H. Koesuka and T. Ando, *Appl. Phys. Lett.*, 1986, **49**, 1210.
19 F. A. Cotton, *Chemical applications of group theory*, 2nd edn., John Wiley & Sons, Inc, New York, 1971.